J|A|C|S
ARTICLES
Published on Web 04/04/2002

Conformational Characterization of Lanthanide(III)−DOTA Complexes by ab Initio Investigation in Vacuo and in Aqueous Solution

Ugo Cosentino,*,† Alessandra Villa,†,⊥ Demetrio Pitea,† Giorgio Moro,‡ Vincenzo Barone,§ and Alessandro Maiocchi||

Contribution from the Dipartimento di Scienze dell'Ambiente e del Territorio (DISAT), Università degli Studi di Milano-Bicocca, Piazza della Scienza 1, 20126 Milano, Italy, the Dipartimento di Biotecnologie e Bioscienze (BTBS), Università degli Studi di Milano-Bicocca, Piazza della Scienza 2, 20126 Milano, Italy, the Dipartimento di Chimica, Università Federico II, Complesso Universitario di Monte S. Angelo, Via Cintia, 80126 Napoli, Italy, and the Bracco SpA, Via E. Folli 50, 20134 Milano, Italy

Received December 3, 2001

Abstract: The conformational behavior of four $[Ln(DOTA)(H_2O)]^-$ systems (Ln = La, Gd, Ho, and Lu) has been characterized by means of ab initio calculations performed in vacuo and in aqueous solution, the latter by using the polarizable continuum model (PCM). Calculated molecular geometries and conformational energies of the $[Ln(DOTA)(H_2O)]^-$ systems, and interconversion mechanisms, barriers, and ^{13}C NMR spectra of the $[Lu(DOTA)]^-$ complex are compared with experimental values. For each system, geometry optimizations, performed in vacuo and in solution at the HF/3-21G level and using a $46+4f^n$ core electron effective core potential (ECP) for lanthanides, provide two minima corresponding to a square antiprismatic (**A**) and an inverted antiprismatic (**IA**) coordination geometry. All the systems are nonacoordinated, with the exception of the **IA** isomer of the Lu complex that, from in solution calculations, is octacoordinated, in agreement with experimental data. On comparing the in vacuo relative free energies calculated at different theory levels it can be seen that the nonacoordinated species dominates at the beginning of the lanthanide series while the octacoordinated one does so at the end. Furthermore, on passing along the series the **IA** isomer becomes less and less favored with respect to **A** and for the Lu complex a stabilization of the **IA** isomer is observed in solution (but not in vacuo), in agreement with the experimental data. Investigation of the **A↔IA** isomerization process in the $[Lu(DOTA)]^-$ system provides two different interconversion mechanisms: a single-step process, involving the simultaneous rotation of the acetate arms, and a multistep path, involving the inversion of the cyclen cycle configuration. While in vacuo the energy barrier for the acetate arm rotation is higher than that involved in the ring inversion (23.1 and 13.1 kcal mol^{-1} at the B3LYP/6-311G** level, respectively), in solution the two mechanisms present comparable barriers (14.7 and 13.5 kcal mol^{-1}), in fairly good agreement with the experimental values. The NMR shielding constants for the two isomers of the $[Lu(DOTA)]^-$ complex have been calculated by means of the ab initio GIAO and CSGT methods, and using a 46-core-electron ECP for Lu. The calculated ^{13}C NMR chemical shifts are in close agreement with the experimental values (rms 3.3 ppm, at the HF/6-311G** level) and confirm the structural assignment of the two isomers based on experimental NMR spectra in solution. The results demonstrate that our computational approach is able to predict several physicochemical properties of lanthanide complexes, allowing a better characterization of this class of compounds for their application as contrast agents in medical magnetic resonance imaging (MRI).

1. Introduction

The use of contrast agents in magnetic resonance imaging (MRI) has become an important tool in modern medical diagnostics. Contrast agents significantly improve the image contrast by enhancing the nuclear magnetic relaxation rates of the water protons in the tissues where they are distributed. Due to the high magnetic moment (seven unpaired electrons) and the relatively long electronic relaxation time of the metal ion, complexes of the gadolinium ion are currently employed in clinical practice.[1] The efficiency of the relaxation enhancement, i.e., the relaxivity, depends on dipolar interactions between the magnetic moment of the metal ion and the nuclear spins of the

* Author for correspondence. E-mail: ugo.cosentino@unimib.it.
† DISAT, University Milano-Bicocca.
⊥ Current address: Groningen Biomolecular Sciences and Biotecnology Institute (GBB), Department of Biophysical Chemistry, University of Groningen, Nijenborgh 4, 9747 AG Groningen, The Netherlands.
‡ BTBS, University Milano-Bicocca.
§ University Napoli.
|| Bracco SpA.

(1) (a) Caravan, P.; Ellison, J. J.; McMurry, T. J.; Lauffer, R. B. *Chem. Rev.* **1999**, *99*, 2293. (b) Lauffer, R. B. *Chem. Rev.* **1987**, *87*, 901. (c) Aime, S.; Botta, M.; Fasano, M.; Terreno, E. *Chem. Soc. Rev.* **1998**, *27*, 19.

Scheme 1

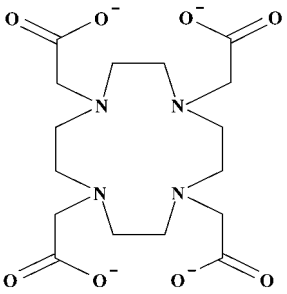

DOTA^{4-}

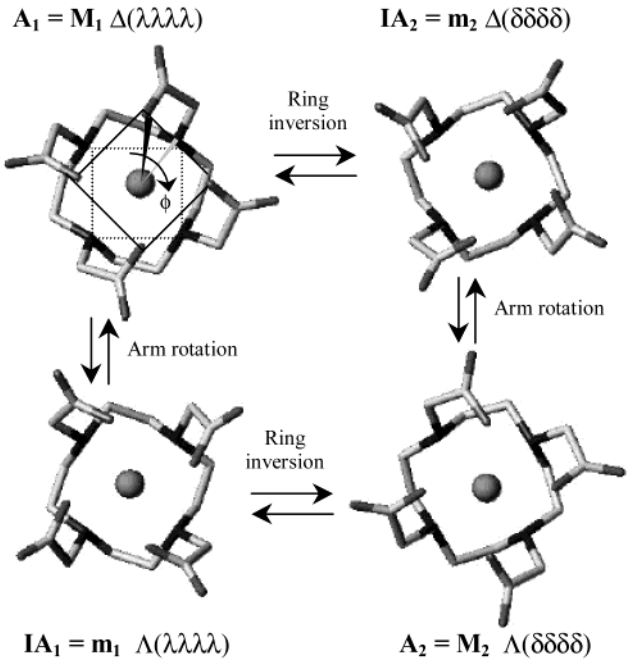

Figure 1. Structures and isomerization processes of the diastereoisomers of [Ln(DOTA)(H_2O)]$^-$ complexes. Symbols Δ and Λ refer to the helicity of the acetate arms, λ and δ to the macrocycle. $\mathbf{M_1}$ and $\mathbf{M_2}$ (equivalent to $\mathbf{A_1}$ and $\mathbf{A_2}$) as well as $\mathbf{m_1}$ and $\mathbf{m_2}$ (equivalent to $\mathbf{IA_1}$ and $\mathbf{IA_2}$) are enantiomeric pairs. The coordinated water molecule has been omitted for clarity. The twist angle, ϕ, between the parallel squares defined by the nitrogen and the acetate oxygen atoms is highlighted.

water protons. Among other effects, the efficiency of the process depends on the number of water molecules bound to the ion, and on their exchange rate with the bulk water.[1]

Because the free ions are very toxic, a prerequisite for their in vivo use is the complexation with polydentate ligands to form compounds of high kinetic and thermodynamic stability in order to prevent dissociation. Polyamino carboxylate (PAC) ligands are widely used in the design of MRI contrast agents because they form particularly stable complexes with lanthanide ions; the leading compound in this class of ligands is DOTA (1,4,7,-10-tetraaza-1,4,7,10-tetrakis (carboxymethyl) cyclododecane). (Scheme 1).

It is well-known that [Ln(DOTA)]$^-$ complexes exist as two enantiomeric pairs of diasteroisomers. In fact, these complexes present two sources of helicity (Figure 1): one due to the four five-membered rings formed by the binding of the acetate arms to the ion (absolute configuration Δ or Λ) and the other to the four five-membered rings formed by the binding of the cyclen (absolute configuration $\delta\delta\delta\delta$ or $\lambda\lambda\lambda\lambda$).

The two diastereoisomeric forms, labeled **M** (major) and **m** (minor) on the basis of the relative population in solution determined by NMR analysis, differ in the layout of the acetate arms. In the two isomers the parallel squares, defined respectively by nitrogen and acetate oxygen atoms, are twisted by a ϕ angle of ca. 40° in **M** and 20° in **m**, providing square antiprismatic (**A**) and inverted antiprismatic (**IA**) geometry, respectively. The solid-state X-ray **m**-type structures have been observed for La,[2] while **M**-type structures have been reported for Eu,[3] Gd,[4] Er,[5] Ho,[6] and Lu.[7]

Generally, the ninth coordination site, at a capping position above the plane defined by the four oxygens, is occupied by one water molecule: in solution there is a fast water molecule−bulk solvent exchange, a process that contributes greatly to the system relaxivity.

An analysis of NMR spectra of [Ln(DOTA)]$^-$ complexes in solution[8,9] showed that (i) the relative concentration of the two isomers is affected by the nature of the central metal ion, the relative stability of the **M** isomer with respect to **m** increasing along the lanthanide series and (ii) for the heaviest lanthanides (from Er to Lu) the conformational equilibrium **M**↔**m** involves the octa-coordinated **m′** species, in which the coordinated water molecule is depleted. Moreover, it was recently observed in DOTA-like complexes[10] that the coordinated water molecule in the two isomers presents different exchange rates with the bulk solvent: thus, the overall exchange rate of the complex is significantly affected by the diastereoisomeric composition.

Theoretical investigation represents a valid tool to an understanding of the structures and dynamics of lanthanide complexes, and to assess those stereoelectronic factors that can lead to compounds with desired properties. In the case of Gd complexes, the long electronic relaxation time of the metal ion prevents any observation of NMR spectra, and for this reason their solution structures and properties have to be deduced from the NMR spectra of complexes with other lanthanides. Theoretical calculations provide direct information on gadolinium systems as well as on those dynamic processes that are too fast to be observed on the NMR time scale, such as the water exchange process.

Previously,[11] we investigated the in vacuo conformational behavior of gadolinium complexes with different PAC ligands and with ligands containing amidic, alcoholic, and phosphinic coordinating groups by means of ab initio methods. Moreover,[11]

(2) Aime, S.; Barge, A.; Benetollo, F.; Bombieri G.; Botta, M.; Fulvio, U. *Inorg. Chem.* **1997**, *36*, 4287.
(3) Spirlet, M. R.; Rebizant, J.; Desreux, J. F.; Loncin, M. F. *Inorg. Chem.* **1984**, *23*, 359.
(4) (a) Dubost, J. P.; Legar, J. M.; Langlois, M. H.; Meyer, D.; Schaefer, M. *C. R. Acad. Sci. Paris, Ser. 2* **1991**, *312*, 349. (b) Chang, C. A.; Francesconi, L. C.; Malley, M. F.; Kumar, K.; Gougoutas, J. Z.; Tweedle, M. F.; Lee, D. W.; Wilson, L. J. *Inorg. Chem.* **1993**, *32*, 3501.
(5) Jin, T.; Wang, X.; Xu, G.; Ma, Z.; Ling, H. *Gaodeng Xuexiao Huaxue Xuebao* **1991**, *12*, 999.
(6) Benetollo, F.; Bombieri, G.; Aime, S.; Botta, M. *Acta Crystallogr.* **1999**, *C55*, 353.
(7) Aime, S.; Barge, A.; Botta, M.; Fasano, M.; Ayala, J. D.; Bombieri, G. *Inorg. Chim. Acta* **1996**, *246*, 423.
(8) Aime, S.; Botta, M.; Fasano, M.; Marques, M. P. M.; Geraldes, C. F. G. C.; Pubanz, D.; Merbach, A. E. *Inorg. Chem.* **1997**, *36*, 2059.
(9) Hoeft, S.; Roth, K. *Chem. Ber.* **1993**, *126*, 869.
(10) Dunand, F. A.; Aime, S.; Merbach, A. E. *J. Am. Chem. Soc.* **2000**, *122*, 1506.
(11) (a) Cosentino, U.; Moro, G.; Pitea, D.; Villa, A.; Fantucci, P. C.; Maiocchi, A.; Uggeri, F. *J. Phys. Chem. A* **1998**, *102*, 4606. (b) Villa, A.; Cosentino, U.; Pitea, D.; Moro, G.; Maiocchi, A. *J. Phys. Chem A* **2000**, *104*, 3421.

we performed the parametrization of the Gd−ligand interactions within molecular mechanics force-fields starting from ab initio calculations.

Due to their specific applications, the modeling of these systems requires the investigation of their behavior in solution. The continuum approach[12] offers a straight methodology for including solvent effect in the study of complex systems. In particular, the polarizable continuum model (PCM)[13] offers a balanced and theoretically sound treatment of all solute−solvent interactions at a very reasonable computational cost, even at ab initio level. Recently, the structural and thermodynamic properties of lanthanide aquo-ions have been reproduced accurately by means of PCM ab initio calculations;[14] the Poisson−Boltzmann continuum solvation model was used to include surrounding effects in the investigation of the $[Y(DOTA)]^-$ system.[15]

This paper concerns the investigation of the conformational behavior of $[Ln(DOTA)]^-$ systems by means of ab initio computations performed both in vacuo and in aqueous solution and indicates which molecular properties are significantly affected by the solvation and which are only marginally perturbed by the environment. Calculated molecular geometries, and conformational energies of four $[Ln(DOTA)(H_2O)]^-$ systems (Ln = La, Gd, Ho, and Lu), and interconversion mechanisms, energetic barriers, and ^{13}C NMR spectra of the $[Lu(DOTA)]^-$ system are compared with experimental values. We demonstrate that reliable computational tools are available to predict several physicochemical properties of lanthanide complexes, and this is clearly evident through the proven accuracy of our computational approach.

2. Computational Methods

Molecular Geometries and Energies. In all calculations, the quasi relativistic effective core potential (ECP) of Dolg et al.[16] and the related [5s4p3d]-GTO valence basis sets are used for lanthanides. This ECP includes $46+4f^n$ electrons in the core, leaving the outermost 11 electrons to be treated explicitly.

Full geometry optimizations of the two isomers of the $[Ln(DOTA)(H_2O)]^-$ systems (Ln = La, Gd, Ho, and Lu) were performed both in vacuo and in aqueous solution; the corresponding octa-coordinated $[Ln(DOTA)]^-$ systems were also optimized in vacuo with C_4 symmetry constraint.[17] On the grounds of our previous experience,[11] geometry optimizations were performed at the HF level using the 3-21G basis set for the ligand atoms. On the optimized structures, single point energy calculations were performed at the HF and DFT (B3LYP functional) levels, by using the 6-31G* and the 6-311G** basis sets for the ligand.[18]

For the different species involved in the considered equilibria, namely, **A**, **A′**+H_2O, **IA**, and **IA′**+H_2O (octacoordinated species are labeled with a prime), the relative free energies with respect to **A** were calculated in vacuo at the HF/3-21G level, including non-potential-energy (NPE) contributions (that is, zero point energy and thermal terms) obtained by frequency analysis. Only in the case of Gd were the calculations performed also at the HF/6-31G* level on the geometries optimized at the same level. Due to the considerable effort involved in calculating second derivatives, an approximated procedure was adopted to estimate the NPE terms at higher theory levels.[19] Corrections for basis set superposition error (BSSE) were taken into account by the standard counterpoise method[18] in the case of equilibria involving depletion of the water molecule from the coordination cage.

Energy barriers and transition states for the **A′↔IA′** isomerization process in the $[Lu(DOTA)]^-$ system were calculated in vacuo at the HF/3-21G level by means of the synchronous transit-guided quasi-Newton method.[20] The nature of the saddle points was characterized by frequency analysis and single point energies at the HF and B3LYP levels with the 6-31G* and 6-311G** basis sets were calculated for all the critical points, both in vacuo and in aqueous solution.

Solvent effects were evaluated by using the Gaussian98[21] implementation of the PCM. In particular, we selected the C−PCM variant[22] that, employing conductor rather than dielectric boundary conditions,[23] allows a more robust implementation. In line with the united atom topological model (UATM),[24] the solute cavity is built as an envelope of spheres centered on atoms or atomic groups with appropriate radii. For lanthanides, the previously parametrized radii[14] were used, neglecting the lanthanide dispersion and repulsion parameters due to their negligible influence in aqueous solution. As usual,[24] all the UATM radii were scaled by 1.2 factor in the calculations of electrostatic contributions, while the unscaled values were used to calculate other contributions. To avoid convergence problems during geometry optimizations, the linear search in the Berny algorithm was removed and the nonelectrostatic contributions to the energy and energy gradient, that is the cavitation, dispersion, and repulsion contributions, were omitted. Final free energies, obtained from single point calculations at optimized geometries in solution, include both electrostatic and nonelectrostatic contributions. It must be remembered that the PCM results have free energies status;[12] thus, in the following they will be referred to as C−PCM free energies, G^{sol}.

NMR Shielding Tensor Calculations. The NMR shielding tensors of the two isomers of the diamagnetic $[Lu(DOTA)]^-$ complex were calculated in vacuo and in aqueous solution at the HF and B3LYP levels using the PCM implementation[25] of the CSGT[26] and GIAO[27] methods. Calculations were performed on the geometries optimized in

(12) Tomasi, J.; Persico, M. *Chem. Rev.* **1994**, *94*, 2027.
(13) Amovilli, C.; Barone, V.; Cammi, R.; Cances, E.; Cossi, M.; Mennucci, B.; Pomelli, C. S.; Tomasi, J. *Adv. Quantum Chem.* **1998**, *32*, 227.
(14) Cosentino, U.; Villa, A.; Pitea, D.; Moro, G.; Barone V. *J. Phys. Chem. B* **2000**, *104*, 8001.
(15) (a) Jang, Y. H.; Blanco, M.; Dasgupta, S.; Keire, D. A.; Shively, J. E.; Goddard, W. A., III *J. Am. Chem. Soc.* **1999**, *121*, 6142. (b) An exhaustive review of computational studies on Gd(III) systems can be found in: Sulzle, D.; Platzek, J.; Raduchel, B.; Schmitt-Willich, H. *The Chemistry of Contrast Agents in Medical Magnetic Resonance Imaging*; Merbach, A. E., Toth, E., Eds.; Wiley: New York, 2001; pp 281−313.
(16) Dolg, M.; Stoll, H.; Savin, A.; Preuss, H. *Theor. Chim. Acta* **1989**, *75*, 173.
(17) In vacuo calculations were performed also on the Nd, Eu, and Yb complexes; molecular geometries and conformational energies, not discussed in the paper, are available as Supporting Information (Tables S1 and S4).
(18) Description of the basis sets and explanation of standard levels of theory can be found in Foresman, J. B.; Frisch, A. E. *Exploring Chemistry with Electronic Structure Methods*, 2nd ed.; Gaussian Inc.: Pittsburgh, PA, 1996.
(19) This procedure is based on the assumptions that NPE terms are not very sensitive to either the lanthanide ion or the computational level. Indeed, a comparison of our results supports these assumptions (Tables S5-S7): at the HF/3-21G level the NPE terms involved in the **A↔IA** process are approximately constant throughout the series, as are those involved in the dissociation of the water molecule from one isomer or the other. Moreover, on comparing the results obtained for Gd at the HF/3-21G and HF/6-31G* levels it can be seen that, for a given equilibrium, the NPE contributions are very similar. This gave us confidence to adopt the following procedure: for a given lanthanide, the values of the NPE contributions at the HF/6-31G* and B3LYP/6-311G* levels (NPE_{Ln}) are assumed equal, and are calculate by the following equation: $NPE_{Ln} = NPE_{Ln/HF3-21G} + (NPE_{Gd/HF6-31G^*} - NPE_{Gd/HF3-21G})$.
(20) (a) Peng, C.; Ayala, P. Y.; Schlegel, H. B.; Frisch, M. J. *J. Comput. Chem.* **1996**, *17*, 49. (b) Peng, C.; Schlegel, H. B. *Isr. J. Chem.* **1994**, *33*, 449.
(21) Frisch, M. J.; Trucks, G. W.; Schlegel, H. B.; Scuseria, G. E.; Robb, M. A.; Cheeseman, J. R.; Zakrzewski, V. G.; Montgomery, J. A., Jr.; Stratmann, R. E.; Burant, J. C.; Dapprich, S.; Millam, J. M.; Daniels, A. D.; Kudin, K. N.; Strain, M. C.; Farkas, O.; Tomasi, J.; Barone, V.; Cossi, M.; Cammi, R.; Mennucci, B.; Pomelli, C.; Adamo, C.; Clifford, S.; Ochterski, J.; Petersson, G. A.; Ayala, P. Y.; Cui, Q.; Morokuma, K.; Malick, D. K.; Rabuck, A. D.; Raghavachari, K.; Foresman, J. B.; Cioslowski, J.; Ortiz, J. V.; Stefanov, B. B.; Liu, G.; Liashenko, A.; Piskorz, P.; Komaromi, I.; Gomperts, R.; Martin, R. L.; Fox, D. J.; Keith, T.; Al-Laham, M. A.; Peng, C. Y.; Nanayakkara, A.; Gonzalez, C.; Challacombe, M.; Gill, P. M. W.; Johnson, B. G.; Chen, W.; Wong, M. W.; Andres, J. L.; Head-Gordon, M.; Replogle, E. S.; Pople, J. A. *Gaussian 98*, revision A.7; Gaussian, Inc.: Pittsburgh, PA, 1998.
(22) Barone, V.; Cossi, M. *J. Phys. Chem. A* **1998**, *102*, 1995.
(23) Klamt, A.; Schüürmann, G. *J. Chem. Soc., Perkin Trans* **1993**, *2*, 799.
(24) Barone, V.; Cossi, M.; Tomasi, J. *J. Chem. Phys.* **1997**, *107*, 3210.

Table 1. Values of the Main Geometrical Parameters of Experimental and Calculated (in Vacuo and in Aqueous Solution) Structures of the Two Isomers of $[Ln(DOTA)(H_2O)]^-$ Complexes[a]

	A isomer			**IA** isomer		
	HF/3-21G in vacuo	HF/3-21G in solution	exptl	HF/3-21G in vacuo	HF/3-21G in solution	exptl
La						
La−O	2.449 (0.037)	2.477 (0.017)		2.459(0.035)	2.491 (0.011)	2.492 (0.010)[b]
La−N	2.827 (0.020)	2.774 (0.014)		2.831(0.014)	2.763 (0.010)	2.769 (0.012)
La−O_w[c]	2.635	2.690		2.624	2.708	2.537
La−P_N[d]	1.823	1.738		1.854	1.742	1.809
La−P_O[e]	0.602	0.773		0.607	0.810	0.720
ϕ[f]	37.2 (1.5)	34.2 (0.5)		−27.1 (1.1)	−23.7 (0.5)	−24.2 (1.6)
Gd						
Gd−O	2.334 (0.035)	2.365 (0.018)	2.365 (0.004)[g]	2.341 (0.034)	2.374 (0.018)	
Gd−N	2.751 (0.021)	2.696 (0.015)	2.655 (0.006)	2.772 (0.018)	2.681 (0.012)	
Gd−O_w	2.515	2.609	2.456	2.508	2.682	
Gd− P_N	1.744	1.651	1.633	1.792	1.651	
Gd− P_O	0.625	0.782	0.719	0.637	0.841	
ϕ	39.0 (1.4)	36.8 (0.5)	36.0 (5.8)	−28.2 (1.2)	−25.9 (1.2)	
Ho						
Ho−O	2.292 (0.035)	2.327 (0.019)	2.330 (0.005)[h]	2.298 (0.034)	2.334 (0.018)	
Ho−N	2.739 (0.025)	2.681 (0.017)	2.642 (0.017)	2.764 (0.020)	2.666 (0.016)	
Ho−O_w	2.462	2.570	2.443	2.459	2.684	
Ho− P_N	1.733	1.638	1.608	1.793	1.641	
Ho− P_O	0.617	0.767	0.727	0.635	0.846	
ϕ	39.5 (1.4)	37.6 (0.6)	39.1 (1.3)	−28.1 (1.4)	−26.0 (1.4)	
Lu						
Lu−O	2.245(0.035)	2.280 (0.018)	2.279 (0.007)[i]	2.250 (0.033)	2.267 (0.007)	
Lu−N	2.725(0.027)	2.653 (0.021)	2.614 (0.021)	2.755(0.023)	2.576 (0.008)	
Lu−O_w	2.424	2.583	2.417	2.420	3.238	
Lu− P_N	1.724	1.609	1.585	1.787	1.509	
Lu− P_O	0.610	0.771	0.733	0.622	0.970	
ϕ	40.0 (1.4)	38.5 (0.8)	39.6 (1.3)	−28.7 (1.4)	−26.9 (1.1)	

[a] The average values are reported with standard deviations in parentheses. Distances (angstroms), angles (deg). [b] Reference 2. [c] Distance of Ln from the coordinated water molecule. [d] Distance of Ln from the least-squares plane defined by the N atoms, P_N. [e] Distance of Ln from the least-squares plane defined by the O atoms, P_O. [f] Twist angle between the P_O and P_N planes. [g] Reference 4. [h] Reference 5. [i] Reference 7.

vacuo at the BLYP/6-31G* level with C_4 symmetry constraint. For the NMR shielding constant calculations, two different ECPs were used for the metal ion: the previously quoted ECP by Dolg et al.[16] and the ECP by Cundari and Stevens.[28] The latter includes 46 electrons in the core (1s−4d), leaving the outermost $11+4f^{14}$ electrons to be explicitly described by a [4s4p2d2f] valence basis set. For the ligand atoms, the 6-31G* and the 6-311G** basis sets were used. For chemical shift calculation purposes, NMR shielding tensors of tetramethylsilane (TMS) were calculated at the appropriate level.

In all calculations, a modified version of the Gaussian 98 package[21] was used.

3. Results and Discussion

Molecular Geometries. For each $[Ln(DOTA)(H_2O)]^-$ system, ab initio calculations provide the **A** and the **IA** isomers as minimum energy conformations, both in vacuo and in solution. Table 1 shows the experimental and calculated values of the main geometrical parameters. Comparison with crystallographic structures shows that the experimental coordination geometries are well reproduced at the HF/3-21G level.

The calculated bond distances between the ion and the coordinated ligand atoms decrease along the lanthanide series, both in vacuo and in solution, in agreement with the experimental evidence: this is also the case for the distance between the least-squares planes defined by the four nitrogen atoms, P_N, and the four acetate oxygen atoms, P_O (i.e., the sum of the Ln−P_O and Ln−P_N distances). Thus, decreasing the ionic radius results in a more compact structure of the complex: the consequent steric hindrance in the coordination cage is relieved by a slight increase in ϕ, the twist angle between the P_O and the P_N planes.

The in vacuo optimized structures present Ln−N bond distances longer than the corresponding experimental values, while the Ln−O bonds are close to the experimental ones. In solution, Ln−N distances are shorter and Ln−O distances are slightly increased, providing a general better agreement with the experimental ones, as also highlighted by the Ln−P_N and Ln−P_O values. The simultaneous decreasing of Ln−P_N and increasing of Ln−P_O in solution leads to a deeper embedding of the metal ion in the coordination cage than in vacuo, an effect more relevant for **IA** than for **A**.

The distance between the lanthanide and the coordinated water molecule, Ln−O_w, presents different trends in vacuo and in aqueous solution (Table 1 and Figure 2). The in vacuo optimized geometries are characterized by Ln−O_w distances close to their experimental counterparts and decreasing along the series, reflecting the reduction of the lanthanide ionic radii. However, the closest approach between the water molecule and the metal ion does not involve a stronger interaction between them, as will be discussed below. For a given lanthanide, the two isomers have very similar Ln−O_w distances and are nonacoordinated along the whole series. The oxygen position of the capping water molecule is close to the experimental one; however, in the crystallographic structure of $[Gd(DOTA)(H_2O)]^-$ the water molecule is nearly perpendicular to P_O,[4b] whereas in the calculated structures it is bent and involved in hydrogen bonds with two acetate oxygens.

The coordinated water molecule is bent also in the structures optimized in solution, but it is characterized by a slightly longer

(25) (a) Cammi, R. *J. Chem. Phys.* **1998**, *109*, 3185. (b) Cammi, R.; Mennucci, B.; Tomasi, J. *J. Chem. Phys.* **1999**, *110*, 7627.
(26) Keith, T. A.; Bader, R. F. W. *Chem. Phys. Lett.* **1993**, *210*, 223.
(27) (a) Ditchfield, R. *Mol. Phys.* **1974**, *27*, 789. (b) Wolinki, K.; Hinton, J. F.; Pulay, P. *J. Am. Chem. Soc.* **1990**, *112*, 8251.
(28) Cundari, T. R.; Stevens, W. J. *J. Chem. Phys.* **1993**, *98*, 5555.

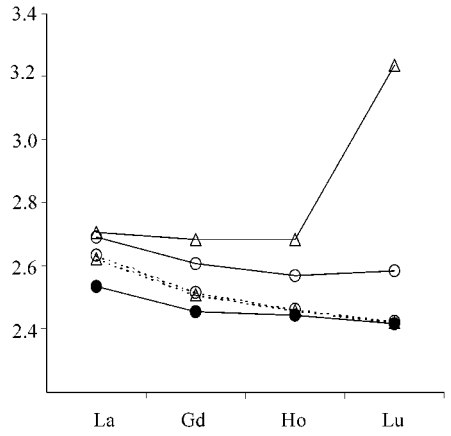

Figure 2. Experimental (●), and in vacuo (- -), and in aqueous solution (—) calculated values of the distance between the lanthanide ion and the coordinated water molecule (Ln−O_w, Å) in the **A** (○) and **IA** (△) isomers of $[Ln(DOTA)(H_2O)]^-$ systems.

Ln−O_w distance (Figure 2). In the **A** isomer, the Ln−O_w distance decreases, passing from La (2.69 Å) to Lu (2.57 Å). In **IA**, the Ln−O_w values are longer than in **A** and approximately constant up to Ho (2.70 Å). In the Lu complex, this distance increases dramatically to 3.24 Å and the water molecule is no longer coordinated to the metal ion, but it still forms hydrogen bonds with two acetate oxygens.

As previously discussed, also in solution the decreasing of the ionic radius along the lanthanide series allows a closer approach between one water molecule and the metal ion but this effect is now counterbalanced by two other factors: the ion is buried deeper in the coordination cage in solution than in vacuo and the coordinated water molecule interacts not only with the metal ion but also with the bulk water molecules. Moreover, as the ion is more embedded in the coordination cage in **IA** than in **A**, the interaction between the ion and the coordinated water molecule is less effective in **IA**. On going along the series, the ninth coordination site of **IA** becomes less accessible to the water molecule in such a way that there is no sufficient space to arrange this water molecule in the coordination cage of the heaviest lanthanides.

Thus, in agreement with experimental NMR data, the results obtained for the $[Ln(DOTA)(H_2O)]^-$ systems in solution indicate an equilibrium involving the **A** and **IA** nona-coordinated species from La to Ho and the **A** and **IA′** species (nona and octa-coordinated, respectively) for Lu.

Conformational Energies. ^{1}H- and ^{13}C NMR spectra of the whole series of the Ln−DOTA complexes in aqueous solution have shown[8,9] that, with respect to **M**, the relative free energy of **m** increases monotonically along the first part of the lanthanide series, reaches a maximum with Ho and then decreases slightly for the heaviest lanthanides (Er−Lu) (Figure 3). A systematic investigation of temperature and pressure effects on the ^{1}H NMR spectra of the Ln−DOTA systems has revealed that for the heaviest lanthanides the conformational equilibrium **M**↔**m** involves the octa-coordinated **m′** species, in which the coordinated water molecule is depleted.[8]

As a first step, we considered the **A**↔**IA** conformational equilibrium, involving only nona-coordinated species. In agreement with the experimental data, results obtained on in vacuo HF/3-21G optimized geometries show that, with respect to **A**, the relative free energy (Table 2 and Figure 3) of **IA**, $\Delta G°_{298K}$, increases along the series, i.e., the relative stability of **A** increases. However, unlike in the experiments, the stabilization of **IA** in the heaviest lanthanides is not observed and the $\Delta G°_{298K}$ values continue to increase up to Lu. Different methods and basis sets, as well as the inclusion of solvent effects on the in vacuo optimized geometries,[29] cause only a shift in this trend (Figure 3). Also the level of geometry optimization shows negligible effects: for the Gd complex, the HF/6-31G* relative energies of **IA** calculated on the HF/3-21G and HF/6-31G* geometries are 1.62 and 1.72 kcal mol^{-1}, respectively.

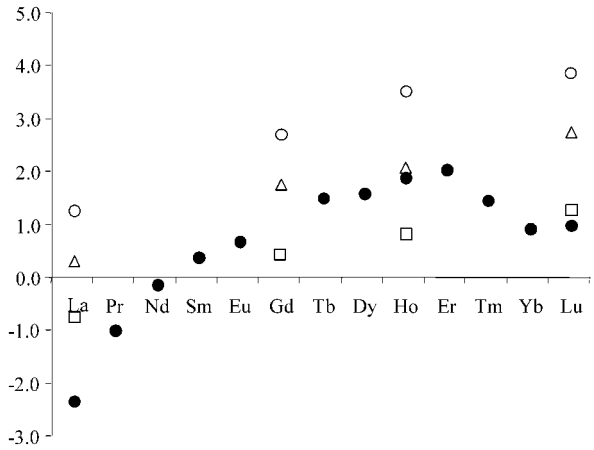

Figure 3. Experimental (●) and in vacuo calculated relative free energies ($\Delta G°_{298K}$) for the **A**↔**IA** equilibrium of $[Ln(DOTA)(H_2O)]^-$ systems: (○) HF/3-21G, (□) HF/6-31G*, (△) B3LYP/6-311G**. Values in kcal mol^{-1}.

Table 2. In Vacuo Relative Free Energies of the **IA** Isomer ($\Delta G°_{298K} = G°_{IA} - G°_{A}$, kcal mol^{-1}) Calculated at Different Levels on HF/3-21G Optimized Geometries of $[Ln(DOTA)(H_2O)]^-$ Systems[a]

	La	Gd	Ho	Lu
HF/3-21G	1.29	2.73	3.55	3.90
HF/6-31G* [b]	−0.71	0.45/0.53[c]	0.87	1.31
B3LYP/6-311G** [b]	0.35	1.78	2.10	2.77
exptl	−2.3	0.7/1.5[d]	1.91	1.0

[a] Experimental $\Delta G°_{298K}$ values are reported.[8] [b] Approximated NPE contributions.[19] [c] Values calculated on HF/6-31G* optimized geometries. [d] Range calculated on the basis of the experimental **A**/**IA** ratio for Eu and Tb complexes at 298 K.[8]

On the basis of these results, we concluded that a simple equilibrium involving only nona-coordinated species was unable to reproduce the experimentally observed stabilization of **IA** in the heaviest lanthanides. Thus, we focused our attention on equilibria involving octa- and/or nonacoordinated species. The relative free energies of the different species involved in the equilibria (**A**, **A′**+H_2O, **IA**, and **IA′**+H_2O) with respect to **A** are reported in Table 3 (further details are in Tables S5−S7, Supporting Information); as an example, Figure 4 reports the $\Delta G°_{298K}$ values of the different species calculated at the B3LYP/6-311G** level.

In general, the relative free energy of **IA** increases and that of the octacoordinated species (**A′**+H_2O and **IA′**+H_2O) decreases along the lanthanide series. At all computational levels the most stable species from La to Gd are nonacoordinated (**A**↔**IA** equilibrium). From Ho to Lu the prevalent species

(29) C−PCM relative free energies of **IA** with respect to **A** in $[Ln(DOTA)(H_2O)]^-$ systems (Ln = La, Gd, and Lu) calculated on the in vacuo optimized geometries are: −2.61, −0.92, and 1.49 (HF/3-21G) and −6.10, −4.59, and −3.03 (HF/6-31G*) kcal mol^{-1}.

Table 3. In Vacuo Relative Free Energies ($\Delta G°_{298K}$) of the **A′**+H_2O, **IA**, and **IA′**+H_2O Species with Respect to **A** of [Ln(DOTA)(H_2O)]$^-$ Systems[a]

		HF/3-21G	HF/6-31G* [b]	B3LYP/6-311G** [b]
La	**A**	**0**	**0**	**0**
	A′+H_2O	3.27	3.70	3.84
	IA	**1.28**	**−0.71**	**0.35**
	IA′+H_2O	4.71	3.36	4.68
Gd	**A**	**0**	**0**	**0**
	A′+H_2O	1.88	2.25	2.64
	IA	**2.73**	**0.45**	**1.78**
	IA′+H_2O	3.48	2.28	3.95
Ho	**A**	0	**0**	**0**
	A′+H_2O	**−0.12**	0.38	0.81
	IA	3.55	**0.87**	**2.10**
	IA′+H_2O	**2.72**	1.59	3.27
Lu	**A**	0	0	0
	A′+H_2O	**−1.16**	**−0.68**	**−0.20**
	IA	3.91	1.31	**2.77**
	IA′+H_2O	**1.99**	**1.20**	3.04

[a] All quantities in kcal mol^{-1}. For each isomer, the value of the prevalent species is highlighted in bold. [b] Approximated NPE contributions.[19]

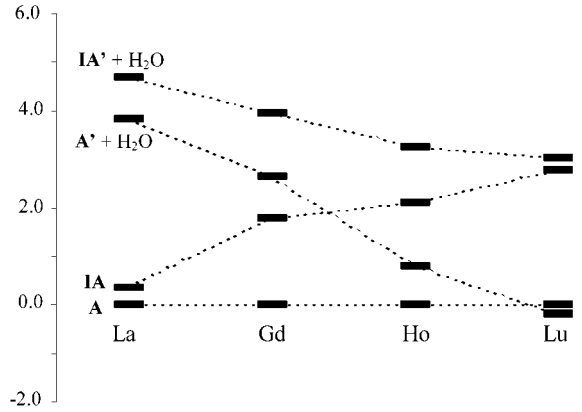

Figure 4. Relative free energies ($\Delta G°_{298K}$, kcal mol^{-1}) with respect to the **A** isomer of the **A′**+H_2O, **IA**, and **IA′**+H_2O species calculated in vacuo at the B3LYP/6-311G** level for the [Ln(DOTA)(H_2O)]$^-$ systems.

depend on the computational level, and due to the reduction of the energetic differences between the species, also the octa-coordinated species are involved in the equilibria, as supported by the experimental findings. The in vacuo calculated relative free energies are reported in Figure 5a. The agreement with the experimental data is fairly good but, once again, the calculated trend does not present the stabilization of the **IA** form observed experimentally for the heaviest lanthanides.

The dissociation free energy of the coordinated water molecule calculated in vacuo decreases along the series, passing from 3.8 (La) to −0.2 (Lu) kcal mol^{-1} (B3LYP/6-311G** results for the **A** isomer, Table 3). Thus, the decreasing of the Ln-O_w bond distances previously stated does not correspond to a stronger binding of the water molecule, but to the decrease of the lanthanide radius that allows a closer approach of the water molecule. Moreover, for the same lanthanide, **IA** presents a less favorable interaction (by about 0.5 kcal mol^{-1}) with the water molecule than **A**, reflecting a greater crowding around the coordination sphere in this isomer.

The C-PCM relative free energies, ΔG^{sol}, calculated in aqueous solution on the C-PCM/3-21G optimized structures are reported in Table 4 and Figure 5b. Here the energetic trend agrees with the experimental one i.e., the relative energy of **IA** increases along the series up to Ho and then moderately

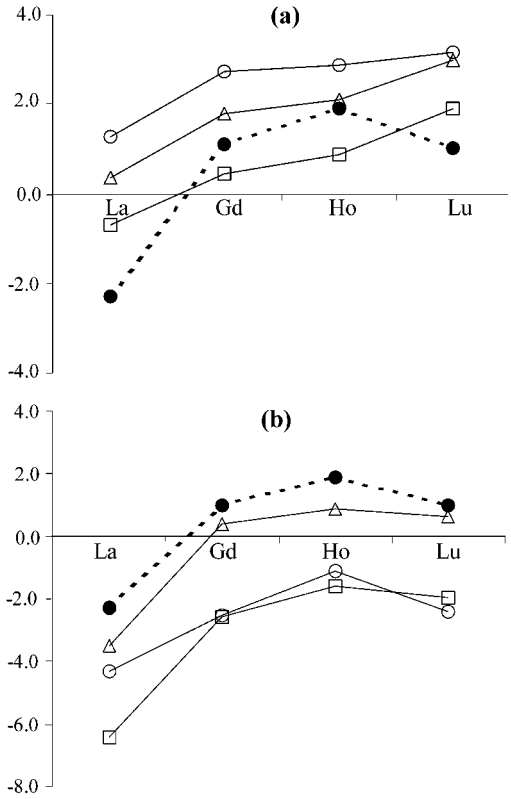

Figure 5. Conformational equilibrium in [Ln(DOTA)(H_2O)]$^-$ systems: (a) *in vacuo* relative free energies ($\Delta G°_{298K}$); (b) in aqueous solution C-PCM relative free energies (ΔG^{sol}). (●) Experimental; (○) HF/3-21G; (□) HF/6-31G*; (△) B3LYP/6-311G**. Values in kcal mol^{-1}.

Table 4. C−PCM Relative Free Energies in Aqueous Solution of the **IA** Isomer ($\Delta G^{sol} = G_{IA}{}^{sol} - G_A{}^{sol}$, kcal mol^{-1}) Calculated on C-PCM HF/3-21G Optimized Geometries of [Ln(DOTA)(H_2O)]$^-$ Systems

	La	Gd	Ho	Lu
HF/3-21G	−4.31	−2.51	−1.10	−2.39
HF/6-31G*	−6.42	−2.55	−1.59	−1.94
B3LYP/6-311G**	−3.51	0.41	0.89	0.65

decreases. This is true at all the considered computational levels, and the B3LYP/6-311G** values present the best quantitative agreement with the experimental ones.

The stabilization in solution of the **IA** isomer for the heaviest lanthanides can be ascribed to the different behavior of the capping water molecule in vacuo and in solution. In vacuo this water molecule is coordinated to the ion in both the isomers along the whole series, thus providing a nearly constant contribution to the energy of the systems. On the contrary, in solution the water molecule interacts in a different way with the two isomers: while the coordination cage of **A** always allows an effective coordination of the water molecule, the steric crowding in **IA** forces the water molecule to leave the coordination site in the heaviest lanthanides. The depletion of this water molecule brings about the release of the steric repulsions in the coordination cage and the formation of effective hydrogen bonds between the water molecule and the acetate oxygens, resulting in the observed stabilization. Thus, the balance between attractive (with the ion, the ligand oxygen atoms, and the bulk) and repulsive (within the first coordination sphere) interactions felt by the water molecule, tunes the position

of the capping water molecule in the coordination cage and affects the relative stability of the species.

Finally, comparison with the in vacuo results reveals that the solvation has a significant effect on the isomeric composition, favoring the **IA** isomer. This effect is mainly due to the different polarity of the two isomers. The **IA** isomer is more polar[30] than **A** and, consequently, is more stabilized by polar solvents. Indeed, the different polarity of the two forms is due to the different orientation of the carboxylic groups in the two isomers: in **A**, the C═O groups are nearly parallel to the P_O plane (the angle between the C═O bond and P_O being 5−10°) while in **IA** they form, on average, an angle of 30° with P_O contributing significantly to the molecular dipole moment. The influence of solvation on the isomeric composition has also been observed experimentally in the case of the [Ce(DOTA)]$^-$ complex, where the **IA** isomer is favored on passing from less polar solvents to water.[8]

Interconversion Process. It was shown experimentally[8,9,31,32] that the interconversion between the two isomers can proceed along two different pathways: (*i*) a rotation of the acetate arms, leading to a Δ→Λ configurational change; (*ii*) an inversion of the cyclen cycle configuration, leading to a *δδδδ*→*λλλλ* change. An analysis of the ^{1}H NMR EXSY spectra of [Eu(DOTA)-$(H_2O)]^-$ [9] and of variable temperature ^{1}H NMR spectra of Pr and Nd complexes[31] has shown that for lighter lanthanides the process involving arm rotation is faster than ring inversion. The quantitative analysis of 2D-EXSY spectra of the Yb complex[32] has shown that the two processes proceed at comparable rates and are characterized by close activation parameters (for the **M**→**m** process: $\Delta H^{\#}$ equal to (*i*) 18.9 ± 1.9 and (*ii*) 19.1 ± 3.6 kcal mol^{-1}, respectively). The activation parameters for the **M**→**m** interconversion of [Lu(DOTA)]$^-$ ($\Delta H^{\#} = 16.6 \pm 0.2$ kcal mol^{-1}) were determined by complete band shape analysis of the variable temperature ^{13}C NMR spectra;[7] however, this analysis did not allow any discrimination between the two different mechanisms.

The calculations of the interconversion process were performed on the octa-coordinated isomers of the [Lu(DOTA)]$^-$ system, **A′** and **IA′**. Results on in vacuo HF/3-21G optimized geometries (Table 5 and Figure 6) confirm both interconversion paths. The cyclen cycle inversion involves a multistep process: at each step, one cycle at a time changes its conformation from a *g*+ to a *g*- conformation, passing through a transition state (TS_R) where the NCCN moiety adopts an eclipsed disposition. Assuming the rate determining step to be the passage between **A′** and the first intermediate, I_{R1}, the barrier for the ring inversion path is the one associated with TS_{R1}.

Conversely, the acetate arm rotation is a single-step process, involving the simultaneous rotation of the four acetates: several attempts to search for a multistep path, involving the rotation of one arm at a time, have not provided any results. In the transition state (TS_A), the four cycles involving the NCCO moieties adopt a nearly planar conformation.

The barrier for the ring inversion path (TS_{R1}), calculated in vacuo at the HF/3-21G level, is almost 20 kcal mol^{-1} lower than that involved in the acetate path (TS_A); the difference reduces to 15 kcal mol^{-1} when NPE terms are included; the B3LYP/6-311G** results reduce this gap further, to 10 kcal mol^{-1}.

Table 5. In Vacuo Relative Energies (ΔE) and in Aqueous Solution C-PCM Relative Free Energies (ΔG^{sol}) of Minima, Intermediates (**I**), and Transition States (TS) Involved in the **A′↔IA′** Interconversion Process of [Lu(DOTA)]$^-$ (Values in kcal mol^{-1})

		ΔE in vacuo		ΔG^{sol} in solution
		HF/3-21G	B3LYP/6-311G**	B3LYP/6-311G**
		Ring Inversion		
A′	+/+/+/+[a]	0	0	0
TS_{R1}	+/0/+/+	16.84[b]/15.43[c]	13.08	14.68
I_{R1}	+/−/+/+	7.57	7.06	4.72
TS_{R2}	+/−/+/0	19.25	15.07	14.10
I_{R2}	+/−/+/−	9.49	5.95	3.75
TS_{R3}	+/−/0/−	18.51	17.18	11.31
I_{R3}	+/−/−/−	10.31	7.63	2.77
TS_{R4}	0/−/−/−	19.48	16.37	11.66
IA′	−/−/−/−	4.45/2.81[c]	2.30	−3.39
		Arm Rotation		
A′		0	0	0
TS_A		36.95[b]/30.81[c]	23.05	13.49
IA′		4.45/2.81[c]	2.30	−3.39

[a] (+) (−) and (0) stay for *gauche*+, *gauche*−, and eclipsed conformation of a NCCN moiety. [b] One negative frequency. [c] Including NPE terms.

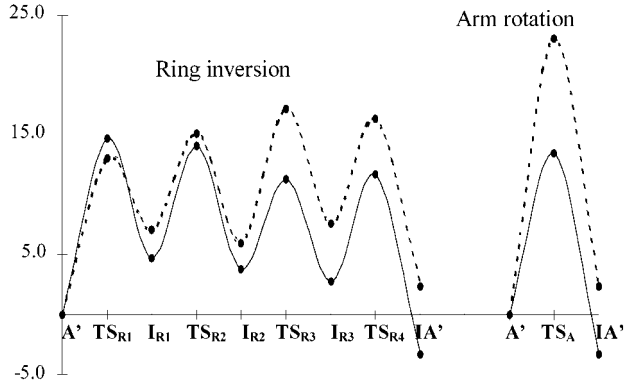

Figure 6. In vacuo B3LYP/6-311G** relative energies (- -, ΔE) and in aqueous solution C−PCM relative free energies (−, ΔG^{sol}) of minima, intermediates (I), and transition states (TS) involved in the **A′↔IA′** interconversion process of [Lu(DOTA)]$^-$. Values in kcal mol^{-1}.

Solvation affects the energy barrier involved in the acetate path significantly, whereas there is a lesser effect on the barrier governing the ring inversion. The comparison of the results obtained in vacuo and in solution at the B3LYP/6-311G** level for TS_{R1} and TS_A provides, respectively, 13.1 and 14.7 kcal mol^{-1} for the ring inversion and 23.1 and 13.5 kcal mol^{-1} for the acetate rotation. As previously discussed, the effect of solvation can be partially ascribed to the different polarity of the intermediates and the transition states involved in the processes. With respect to **A′** ($\mu = 12.3$ D at the B3LYP/6-311G** level), TS_A presents a dipole moment ($\mu = 16.9$ D) higher than TS_{R1} ($\mu = 13.1$) and this fact can justify the greater stabilization of TS_A (9.6 kcal mol^{-1}) with respect to TS_{R1} (−1.6 kcal mol^{-1}) passing from vacuum to aqueous solution.

As a result, the barriers calculated in solution (14.7 and 13.5 kcal mol^{-1}, for the ring inversion and for the acetate rotation, respectively) are similar, as observed experimentally in the case of the Yb complex. Moreover, the calculated values compare well with the experimental ones[7,32] determined for the Yb (18.9

(30) The HF/6-31G* dipole moment values (*D*) calculated on the *in vacuo* optimized geometries for the **A** and **IA** isomers of $[Ln(DOTA)(H_2O)]^-$ systems are, respectively, La, 11.0, 16.7; Gd, 11.8, 17.1; Lu, 11.9, 16.8. All the systems have the same reference origin in the lanthanide ion.
(31) Aime, S.; Botta, M.; Ermondi, G. *Inorg. Chem.* **1992**, *31*, 4291.
(32) Jacques, V.; Desreux, J. F. *Inorg. Chem.* **1994**, *33*, 4048.

Table 6. Experimental and Calculated (GIAO method) ^{13}C NMR Chemical Shift Values (δ, ppm) for the Two Octacoordinated Isomers of [Lu(DOTA)]$^{-}$ [a]

	HF/6-31G*		HF/6-311G**	
	A′	**IA′**	**A′**	**IA′**
		In Vacuo		
NCCN	50.5	47.0	53.3	49.2
NC̄CN	51.3	49.0	54.2	51.7
NCC̄O	64.4	59.2	67.7	61.9
NC̄C̄O	177.8	175.0	188.3	184.9
rms[b]	5.3		3.3	
		In Solution		
NCCN	50.1	46.3		
NC̄CN	51.7	49.6		
NCC̄O	63.8	59.1		
NC̄C̄O	183.3	182.1		
rms[b]	4.5			
		Experimental[c]		
	M	**m**		
NCCN	56.9	50.9		
NC̄CN	57.6	55.9		
NCC̄O	67.4	61.5		
NC̄C̄O	182.8	181.7		

[a] Chemical shifts with respect to TMS calculated on in vacuo BLYP/6-31G* optimized geometries. The TMS absolute shielding constants are calculated at the appropriate level on the BLYP/6-31G* optimized geometry. [b] Root-mean-square (ppm) deviations with respect to experimental data. [c] Reference 7.

and 19.1 kcal mol^{-1}, for the two processes, respectively) and the Lu (16.6 kcal mol^{-1}) complexes.

Finally, we want to highlight that our calculations, performed on octa-coordinated species, did not take into account the possible influence of the coordinated water molecule on the mechanism and the energetic of the process. Hydrogen bond interactions between the coordinated water molecule and the acetate oxygens could stabilize a multistep pathway for the acetate arm rotation or could influence the height of the calculated barriers. Despite this, our results are in qualitative agreement with the experimental data, thus suggesting that either the coordinated water molecule plays a marginal role in this process or that the interconversion process involves, at least in the case of the heaviest lanthanides, octa-coordinated species.

NMR Shielding Constants. Considering all the paramagnetic [Ln(DOTA)]$^{-}$ complexes where ^{1}H NMR spectroscopy revealed two isomers, one isomer had greater paramagnetic shift than the other and, on the basis of the relative population in solution, this was labeled **M** (for major), the second was labeled **m** (for minor). The structures in solution of these isomers were determined on the basis of an analysis of the dipolar shifts in the ^{1}H NMR spectrum of the [Yb(DOTA)]$^{-}$ complex:[31] **M** resulted in a square antiprismatic arrangement (**A**), **m** in an inverted antiprismatic one (**IA**). In the case of the diamagnetic [Lu(DOTA)]$^{-}$ complex, the major isomer **M** was attributed to the square antiprismatic **A** geometry (and **m** to **IA**), by analogy with the results obtained for [Yb(DOTA)]$^{-}$ and according to the **M**-type crystallographic structure[7] of [Lu(DOTA)(H$_2$O)]$^{-}$.

To validate this assignment, the ^{13}C NMR shielding constants of the octa-coordinated **A′** and **IA′** isomers of the [Lu(DOTA)]$^{-}$ complex were calculated. The main results are reported in Table 6 and further details are given in Tables S8 and S9.

Calculation of the NMR shielding constants using the 46+4f^{14} core electron ECP[16] provides inconsistent ^{13}C NMR chemical shifts.[34] On the contrary, the 46 core electron ECP by Cundari and Stevens,[28] that leaves the 4f^{14} electrons in the valence, provides ^{13}C NMR chemical shifts close to the experimental values. A comparison of the HF/6-31G* results obtained from GIAO and CGST calculations, shows that both methods provide comparable results: the root-mean-square (rms, ppm) deviation between chemical shifts calculated in vacuo and those resulting from experimental ^{13}C NMR spectrum is 5.3 and 6.3 ppm, respectively (Table S8, Supporting Information). As the GIAO method presents faster convergence with basis sets with respect to CGST,[33] further calculations were performed by the GIAO method. An improvement in the results is achieved by using better basis sets (rms = 3.3 ppm, at the HF/6-311G** level), the inclusion of electronic correlation does not provide better results (rms = 5.9 ppm, at the B3LYP/6-311G** level). Finally, the inclusion of solvent effects provides only a small improvement (rms = 4.5 ppm at the C-PCM/HF/6-31G* level), highlighting the negligible influence of solvation on the shielding constants of these carbon atoms.

In general, there is a satisfactory agreement between the experimental and the calculated chemical shifts, and the results confirm the experimental assignment of the **M** isomer to the square antiprismatic **A** geometry and of **m** to the inverted antiprismatic **IA** one.

4. Conclusions

Ab initio calculations performed in vacuo on the [Ln(DOTA)(H$_2$O)]$^{-}$ systems are able to capture the main features of these systems when the properties are mainly determined by intramolecular interactions; several properties calculated *in vacuo* are in close agreement with experimental evidences. Thus, when the ionic radius decreases along the lanthanide series the structures become more and more compact and the stability of the octacoordinated species increases with respect to that of the nonacoordinated ones. Moreover, two diastereoisomeric forms have been detected as minimum energy conformations: the **A** isomer, always preferred as nonacoordinated, and the **IA** isomer, nonacoordinated at the beginning of the series and octacoordinated with the heaviest lanthanides. The different behavior of the two isomers along the series is due to the greater sensitivity of **IA** to the steric interactions of the coordinated water molecule with the coordination cage. Furthermore, two paths have been determined for the interconversion process between the isomers: a single-step process involving the simultaneous rotations of the acetates arms, and a multistep process involving the inversion of the cycle. Finally, the ^{13}C NMR chemical shifts calculated in vacuo for the [Lu(DOTA)]$^{-}$ system result in close agreement with the experimental ones, showing the reliability of the computational approach in calculating ^{13}C NMR spectra of complexes of diamagnetic lanthanides with DOTA.

Our results have shown that inclusion of solvent effects is required in order to have a better description of the properties affected by the environment, properties such as the relative energy of the species present in solution and the behavior of

(33) Cheeseman, J. R.; Trucks, G. W.; Keith, T. A.; Frish, M. J. *J. Chem. Phys.* **1996**, *104*, 5497.

(34) The ^{13}C NMR chemical shifts of the **A** isomer of [Lu(DOTA)]$^{-}$ calculated at the HF/6-31G* level by using the CSGT and GIAO methods and the 46+4f^{14} core electron ECP[16] are, respectively, (NCCN) −56.9, and −157.3. (NCCN) −56.8, and −154.0. (NCCO) −58.9, and −141.6. (NCCO) -66.5, and −96.3. The corresponding experimental values are reported in Table 6.

the coordinated water molecule. The different polarities of the species play an important role in determining their relative stability in a high dielectric medium like water, as demonstrated by the results obtained for the conformational energies of the isomers and for the activation energies of the interconversion process. Furthermore, the solvent plays a crucial role in determining the behavior of "weakly" bounded systems, such as the coordinated water molecule. Here, intermolecular interactions with the bulk make the behavior of the coordinated water molecule in the two isomers along the lanthanide series different, as shown by the trend of the Ln-O_w distances calculated in solution.

In conclusion, we are confident that our computational approach provides a reliable description at the molecular level of the processes and mechanisms of these systems, allowing the rational design of new relaxation reagents characterized by optimal values of the most interesting physicochemical properties.

Acknowledgment. The financial support from the Italian National Research Council (CNR Target Project on Biotechnology, Grant n. 01.00265.PF49) is gratefully acknowledged.

Supporting Information Available: Geometrical parameters of the two isomers of $[Ln(DOTA)(H_2O)]^-$ complexes (Ln = Eu, Nd, and Yb) (Table S1). In vacuo total energies (hartree) (Table S2) and C-PCM total free energies (Hartree) (Table S3). In vacuo relative energies of the **IA** isomers (Table S4). In vacuo free energy variations for equilibria involving octa- and nona-coordinated species (Table S5−S7 and Figure S1). GIAO and CSGT ^{13}C NMR chemical shifts in vacuo and in aqueous solution (Tables S8 and S9). Optimized Cartesian coordinates (Å) in vacuo (Tables S10−S25 and S34) and in aqueous solution (Tables S26−S33). This material is available free of charge via the Internet at http://pubs.acs.org.

JA017666T